



Electronic Excited States of the Dihalomethanes, CH_2X_2 ($\text{X}=\text{Cl}, \text{Br}, \text{I}$)

Research Article

Aparna Shastri^{*1}, Anuvab Mandal², Param Jeet Singh¹ and B.N. Jagatap²

¹Atomic and Molecular Physics Division, Bhabha Atomic Research Centre, Mumbai 400085, India

²Homi Bhabha National Institute, Bhabha Atomic Research Centre, Mumbai 400085, India

*Corresponding author: ashastri@barc.gov.in

Abstract. The vacuum ultraviolet (VUV) photoabsorption spectra of the dihalomethanes CH_2X_2 ($\text{X}=\text{Cl}, \text{Br}, \text{I}$) are studied using synchrotron radiation in the energy region 6–11.8 eV ($\sim 49,000$ – $95,200 \text{ cm}^{-1}$). A detailed comparison is made to identify similarities, differences and trends in the spectra and excited state structure of these three molecules. The electronic spectra of the dihalomethanes in this region are dominated by Rydberg series of ns , np and nd type. Quantum defect analysis reveals that the Rydberg series in all the dihalomethanes originate from the four outermost halogen lone pair non-bonding orbitals. On going from Cl to I, the energy difference between the first four ionization potentials decreases which as a consequence leads to spectral congestion and complications in spectral assignments. In all three molecules, several Rydberg transitions are accompanied by vibrational structure. A notable common feature seen in the vibronic structure is the excitation of the ν_3 (C–X symmetric stretch) mode to form extensive progressions. Additionally, the ν_1 (C–H symmetric stretch), ν_2 (CH_2 bend) and ν_8 (CH_2 wag) modes are observed in CH_2Cl_2 and CH_2I_2 , although they do not form long progressions. Quantum chemical calculations of ground and excited states are used to support the analysis and an improved theory-experiment comparison is provided for CH_2Br_2 .

Keywords. Excited states; Dihalomethanes; Rydberg series; VUV photoabsorption; Vibronic structure

PACS. 33.20.-t

Received: May 5, 2015

Accepted: November 30, 2015

1. Introduction

Dihalomethanes (CH₂X₂, X=F, Cl, Br, I) are currently well recognized to play an important role in several environmental issues such as ozone depletion, tropospheric chemistry and aerosols formation in coastal areas [1]. Investigation of the photochemical processes and atmospheric dynamics involving these molecules requires a thorough understanding of their excited state structure and spectra. There have been relatively few studies reported on the electronic structure and spectra of the dihalomethanes, as compared to the monoalkyl halides, possibly due to increased complexity in their spectra resulting from the presence of two carbon-halogen bonds. This leads to interactions between the lone pairs and local σ^* configurations; an effect which has been observed to be more pronounced in the dibromides and diiodides than the corresponding dichlorides and difluorides [2].

Recently, we have reported systematic studies of the electronic absorption spectra of CH₂X₂ (X=Cl, Br, I) using synchrotron radiation in the energy region 3.5–11.8 eV ($\sim 30,000$ – $95,200$ cm⁻¹) [3–5]. Density functional theory (DFT) calculations of the neutral and ionic ground state geometries and vibrational frequencies were used to assign the observed vibronic structure. Extensive time dependent DFT (TDDFT) calculations of excited states were carried out to aid the interpretation of the Rydberg and valence nature of observed transitions. Assignments were verified and consolidated by a comparative study of the VUV spectra of these molecules with those of their deuterated isotopologues CD₂X₂ (X=Cl, Br, I), which were reported for the first time [3–5]. The main objective of this paper is to provide a comparative study of the spectra of these molecules to augment the understanding of the structure, geometry and vibrational modes of the excited states and the nature of the interactions. It may be mentioned here that the VUV absorption spectrum of CH₂F₂ in the region $< 95,200$ cm⁻¹, as reported by us previously [6], exhibits only a few transitions converging to the first four ionization potentials (IPs). We therefore restrict ourselves to presenting a consolidated view of the electronic absorption spectra of dihalomethanes, CH₂X₂, X=Cl, Br, I, *i.e.*, excluding F, unless otherwise specified.

2. Experimental

Photoabsorption studies are carried out using the Photophysics beamline at the 450 MeV Indus-1 storage ring at the Raja Ramanna Centre for Advanced Technology (RRCAT), Indore, India [7]. The broad band synchrotron radiation is dispersed by a 1 meter Seya-Namioka monochromator, covering the spectral range from $30,000$ – $95,000$ cm⁻¹ with an average resolving power of ~ 1000 . A gas phase experimental station is coupled to the beamline and mechanically isolated by a lithium fluoride (LiF) window, thereby limiting the optical transmission to $< 95,238$ cm⁻¹. Monochromatized synchrotron radiation passes through the 25 cm long gas cell and is detected by a sodium salicylate scintillator coupled to a UV-visible photomultiplier tube. The transmitted intensity through the evacuated cell (I_0) and through the sample (I) are measured and the absorption spectrum is obtained using the well-known Beer-Lambert law: $I(\lambda) = I_0 e^{-n\sigma(\lambda)L}$; where $\sigma(\lambda)$ is the absorption cross section, n is the number density of molecules interacting with the beam and L is the absorption path length. The samples in liquid form are contained in a glass vial connected to the absorption cell by a glass-metal seal and several Swagelok valves. Capacitance gauges are used to accurately measure the sample pressure, which is varied from 10^{-4} to 1 mbar. Several freeze-pump-thaw cycles are performed on the samples to remove volatile impurities before introducing them into the gas cell. Intensities are normalized with respect to the beam current which is recorded at every step of 0.5 Å which decides the accuracy of measurement. Details of the experimental setup have been described in earlier papers [3–5] and references therein.

3. Results and discussion

The ground state molecular orbital (MO) configuration of CH₂Cl₂, CH₂Br₂ and CH₂I₂ is given by [core](1a₁)²(1b₂)²(2a₁)²(1b₁)²(3a₁)²(2b₂)²(4a₁)²(1a₂)²(2b₁)²(3b₂)²; with the order of the highest two occupied MOs being reversed in the case of CH₂Cl₂, *i.e.*, (3b₂)²(2b₁)². The VUV photoabsorption spectra of the three dihalomethanes in the regions 49,000–76,500 cm⁻¹ and 76,500–94,800 cm⁻¹ recorded using synchrotron radiation are shown in Figures 1 and 2 respectively. Rydberg series converging to the first four IPs, *i.e.*, corresponding to excitation of an electron from one of the four highest occupied MOs (HOMOs), are seen [3–5]. Broad band absorptions in the lower energy (UV) region and anomalously high underlying intensity pedestals in the region of the higher Rydberg states, where a considerable drop in absorption intensity is normally expected, have been attributed to valence transitions [3–5].

Theoretical calculations performed using the GAMESS (US) suite of programs [8] on a LINUX based platform are used to support the spectral analysis. Geometry optimization and vibrational frequency calculations of the ground states of the neutral molecules, their cations and the corresponding deuterated isotopologues are performed using the DFT formalism. Vertical excited states are computed using the TDDFT methodology, fixing the molecular geometrical parameters to the optimized ground state values. Further details on the methods and basis sets used may be found elsewhere [3–5]. In what follows, we discuss the comparison of (a) Rydberg series, (b) correlation of the experimental versus theoretical excitation energies and (c) vibronic transitions in the electronic spectra of CH₂Cl₂, CH₂Br₂ and CH₂I₂.

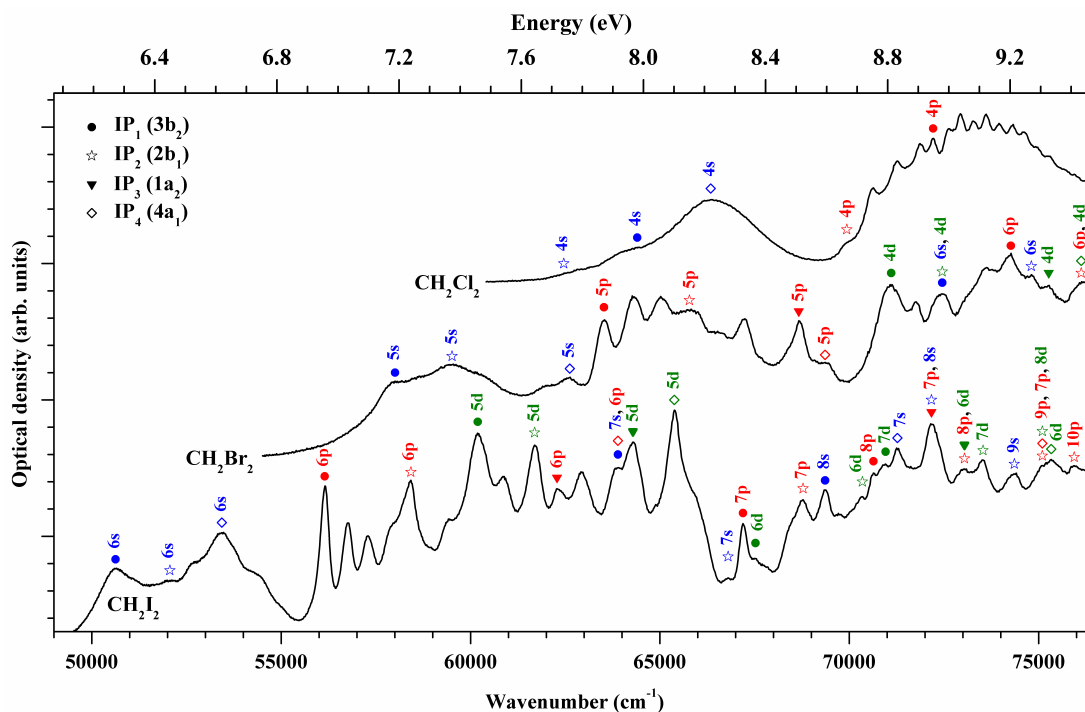


Figure 1. Photoabsorption spectra of dihalomethanes in the region 49,000–76,500 cm⁻¹. *ns* Rydberg series converging to the first three IPs and *np, nd* Rydberg series converging to the first four IPs are marked.

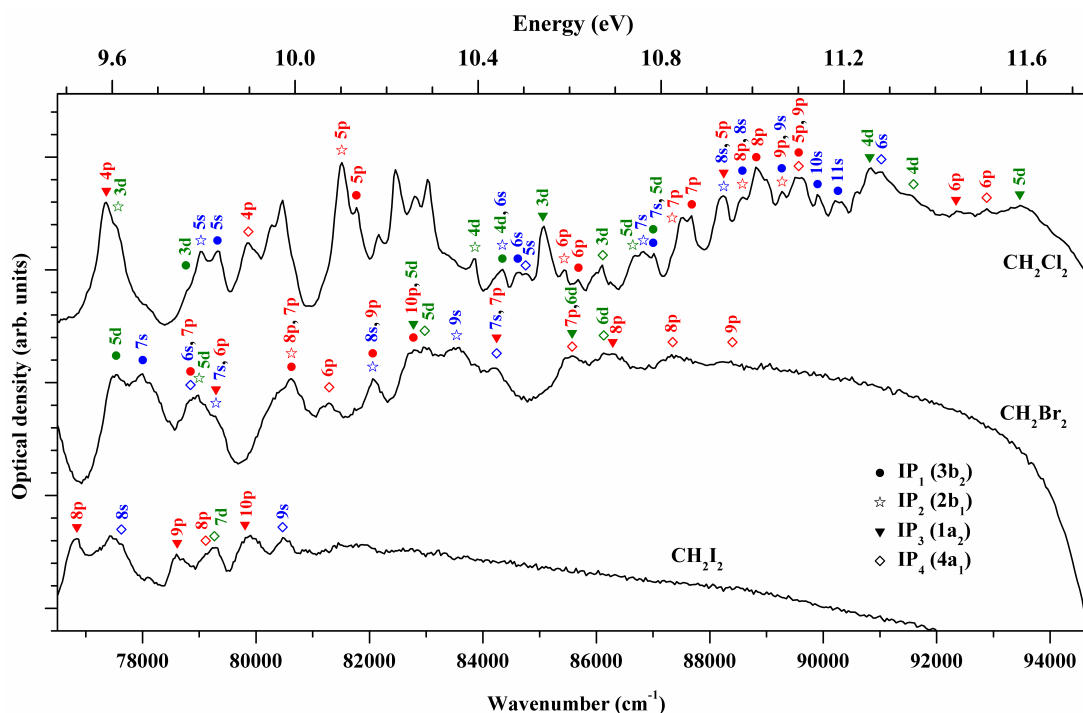


Figure 2. Photoabsorption spectra of dihalomethanes in the region 76,500–94,800 cm⁻¹. *ns* Rydberg series converging to the first three IPs and *np*, *nd* Rydberg series converging to the first four IPs are marked.

(a) Rydberg Series

Rich spectra comprising of Rydberg series of the type *ns*, *np* and *nd* are observed for all three molecules (*cf.* Figures 1 and 2; Tables 1 and 2). The first four IPs are very close in energy leading to severe overlap of their respective Rydberg series, especially for higher principal quantum numbers *n*. Assignment of Rydberg series is carried out on the basis of a quantum defect (QD) analysis using the standard Rydberg formula [3–5]. The experimentally observed average QD values of (*ns*, *np*, *nd*) Rydberg series for CH₂Cl₂, CH₂Br₂ and CH₂I₂ are (2.07, 1.67 and 0.12), (3.02, 2.74 and 1.24) and (4.03, 3.63 and 2.51) respectively. Allowing for small deviations due to the molecular environment, these QDs are in good agreement with the atomic QDs of Cl, Br and I respectively. Comparing the energy differences between two successive IPs, it is observed that for all three molecules, $|IP_2 - IP_1| < |IP_3 - IP_2| > |IP_4 - IP_3|$, where the absolute values have been used in order to take care of the reverse energy ordering of the highest two MOs in CH₂Cl₂. We also observe that the value of the first IP decreases systematically from X = Cl to I, likewise for the second, third and fourth IPs. The observed trends in QDs as well as IPs are consistent with the picture of electron excitation from the halogen lone pair MOs.

The first *ns* Rydberg transitions corresponding to the IP (3b₂) occur at 7.985, 7.192 and 6.277 eV for X=Cl, Br and I respectively, while the first *ns* Rydberg transitions corresponding to the IP (2b₁) occur at 7.7, 7.378 and 6.455 eV for X=Cl, Br and I respectively (*cf.* Figure 1 and Tables 1 and 2). For the third IP (1a₂), the *ns* Rydberg series are forbidden by symmetry, and are hence excluded from Table 2, while the first *ns* series converging to the fourth IP (4a₁) lie at 8.225, 7.764 and 6.625 eV respectively (*cf.* Figure 1 and Table 2). Similar trends can be seen for the *np* and *nd* series as well.

It is further observed that the richest spectrum is obtained for CH₂Cl₂, in which 8 members of the *ns* series ($n = 4$ to $n = 11$), 6 members of the *np* series ($n = 4$ to $n = 9$) and 3 members of the *nd* series ($n = 3$ to $n = 5$) converging to the IP ($3b_2$) are observed distinctly. Similar trends are seen for the next higher IP ($2b_1$). However, in case of the third and fourth IPs, the situation appears to be reversed, with more transitions seen the case of X=Br and I as compared to X=Cl. This may be due to the fact that the higher Rydberg members of CH₂Cl₂ fall very close to or above the higher energy cut-off of the LiF window used in the present experimental arrangement.

Although peak positions of electronic transitions in molecules are not expected to shift with isotopic substitution, small shifts have been observed in the spectra of corresponding deuterated isotopologues [3–5]. This is attributed to the differences in zero point energies between ground and excited states, which is different for different isotopologues.

(b) Correlation of Theoretical and Experimental Excitation Energies

Theoretical values of vertical excited states using the TDDFT methodology are reported by us at the PBE0/aug-cc-pV5Z level of theory for CH₂Cl₂ and CH₂Br₂ [3, 4] and at the PBE0/aug-cc-pVQZ level of theory for CH₂I₂ [5]. At this level of theory, the agreement of theoretical and experimental values is expected to be quite good up to $(-HOMO) + 1$ eV [3–5]. It is pertinent to mention here that correspondence of theoretical and experimental energy values are to be carried out on the basis of the symmetries of initial and final MOs involved in the transition, rather than merely matching of theoretical and experimental values. While this procedure has been followed in CH₂Cl₂ [3] and CH₂I₂ [5], in the case of CH₂Br₂ the earlier work took into account the symmetries of only the initial orbitals and for excitation from a given initial MO, the theoretically predicted transition closest to the experimentally observed Rydberg transition was assigned [4]. This leads to some inconsistencies in assignment of theoretical energies to observed Rydberg series of CH₂Br₂. For example, for a given IP, successive transitions within a particular Rydberg series (*ns*, *np* or *nd*) were assigned to final MOs of different symmetries. Moreover, the molecular geometry used in the calculation was such that the b_1 and b_2 symmetries were interchanged with respect to the convention used in other works. In order to put things in correct perspective and for convenience of comparison, we present here the vertically excited states of CH₂Br₂ predicted using TDDFT along with the corresponding experimentally observed Rydberg series, in which symmetries of initial and final orbitals have been properly considered while making the assignments (*cf.* Tables 3 and 4). It may be noted that for the *ns* series we expect the final MOs to be of a_1 symmetry, while for the *np* and *nd* series the final MOs should be the same within a given series that converges to a particular IP. In this manner, all experimentally observed transitions are correlated with theoretically calculated energies. Tables 3-6 also give the excitation amplitudes (A) for the major orbital excitations ($A > 0.4$) contributing to each transition, oscillator strengths (f) and lambda diagnostic (Λ) values. Revised assignments of theoretical transitions to experimental energies are given in bold type. The Λ value of a transition predicted by the TDDFT calculation denotes the extent of overlap of the initial and final state wavefunctions and may be used as an indication of the Rydberg/valence nature of the excitation [3–5].

Table 1. Rydberg series of the dihalomethanes converging to the first and second IPs ^a

Assignment	IP (3b ₂)			IP (2b ₁)		
	CH ₂ Cl ₂	CH ₂ Br ₂	CH ₂ I ₂	CH ₂ Cl ₂	CH ₂ Br ₂	CH ₂ I ₂
4s	7.985 (1.99)			~7.7 (2.06)		
5s	9.835 (2.01)	7.192 (2.98)		9.798 (2.01)	7.378 (2.99)	
6s	10.491 (2.04)*	8.983 (3.02)*	6.277 (3.93)	10.457 (2.03)*	9.275 (2.95)	6.455 (3.97)
7s	10.787 (2.11)*	9.671 (3.00)	7.921 (4.03)*	10.766 (2.05)*	9.831 (3.13)*	8.282 (3.97)
8s	10.982 (1.98)*		8.600 (4.02)	10.941 (2.01)*	10.174 (3.10)*	8.948 (3.91)*
9s	11.069 (2.14)*				10.357 (3.04)	9.219 (3.98)
10s	11.146 (1.97)					
11s	11.188 (2.03)					
4p	8.953 (1.62)			8.670 (1.73)		
5p	10.138 (1.66)	7.876 (2.73)		10.106 (1.65)*	8.155 (2.71)	
6p	10.624 (1.69)	9.208 (2.78)	6.962 (3.67)	10.592 (1.68)	9.438 (2.77)*	7.244 (3.67)
7p	10.871 (1.71)	9.776 (2.72)*	8.331 (3.53)	10.828 (1.74)	9.996 (2.72)*	8.528 (3.68)
8p	11.012 (1.72)	9.996 (2.90)*	8.758 (3.60)	10.982 (1.66)*		9.056 (3.61)*
9p	11.100 (1.72)*	10.174 (2.73)*		11.069 (1.64)*		9.311 (3.50)*
10p		10.263 (2.73)*				9.415 (3.72)
3d	9.765 (0.08)			9.617 (0.17)		
4d	10.457 (0.11)*	8.816 (1.17)		10.397 (0.16)	8.983 (1.22)*	
5d	10.787 (0.11)*	9.613 (1.13)	7.463 (2.39)	10.742 (0.15)	9.791 (1.21)	7.649 (2.46)
6d			8.372 (2.46)			8.722 (2.38)
7d			8.798 (2.47)			9.117 (2.40)
8d						9.311 (2.50)*

^aQuantum defect values in the parenthesis, *blended lines

Table 2. Rydberg series of the dihalomethanes converging to the third and fourth IPs ^a

Assignment	IP (1a ₂)			IP (4a ₁)			
	IP (eV)	CH ₂ Cl ₂	CH ₂ Br ₂	CH ₂ I ₂	CH ₂ Cl ₂	CH ₂ Br ₂	CH ₂ I ₂
4s					8.225 (2.17)*		
5s					10.508 (2.22)	7.764 (3.04)	
6s					11.286 (2.28)*	9.776 (3.01)*	6.625 (4.14)
7s						10.445 (3.01)*	8.836 (4.19)
8s							9.625 (4.19)
9s							9.977 (4.17)
4p		9.592 (1.69)			9.902 (1.60)		
5p		10.941 (1.65)*	8.514 (2.75)		11.100 (1.59)*	8.600 (2.76)	
6p		11.449 (1.60)	9.831 (2.86)	7.722 (3.66)	11.516 (1.75)	10.079 (2.66)	7.921 (3.73)*
7p			10.445 (2.78)	8.948 (3.72)*		10.610 (2.56)*	9.311 (3.70)*
8p			10.699 (2.84)	9.527 (3.54)		10.830 (2.62)	9.809 (3.74)
9p				9.747 (3.58)		10.960 (2.67)	
10p				9.895 (3.43)			
3d		10.546 (0.09)			10.677 (0.08)*		
4d		11.260 (0.09)*	9.332 (1.31)		11.356 (0.14)*	9.438 (1.30)	
5d		11.588 (0.09)	10.263 (1.21)	7.971 (2.54)		10.288 (1.33)	8.106 (2.65)
6d			10.610 (1.24)	9.056 (2.57)*		10.679 (1.32)	9.340 (2.66)
7d							9.828 (2.69)

^aQuantum defect values in the parenthesis, * blended lines

Table 3. Vertical excited states of CH₂Br₂ corresponding to Rydberg series converging to IP(3b₂) = 10.52 eV

Assignment	Observed peak position (eV)	Calculated by TDDFT: PBE0/aug-cc-pV5Z					O–C (eV)
		E (eV)	<i>f</i>	Transition	<i>A</i>	Λ	
5s	7.192	7.025	0.043	3b ₂ → 6a ₁	-0.95	0.30	0.167
6s	8.983*	8.591	0.023	3b ₂ → 8a ₁	-0.88	0.25	0.392
7s	9.671	9.214	0.008	3b₂ → 10a₁	-0.65	0.38	0.457
5p	7.876	8.017	0.001	3b ₂ → 7a ₁	0.98	0.23	-0.141
		8.169	0.019	3b₂ → 5b₂	-0.93	0.37	-0.293
6p	9.208	8.991	0.003	3b₂ → 9a₁	-0.81	0.27	0.216
		8.886	0.029	3b ₂ → 6b ₂	0.90	0.26	0.321
7p	9.776*	9.866	0.112	3b₂ → 11a₁	0.70	0.30	-0.090
		9.543	0.014	3b ₂ → 7b ₂	0.53	0.25	0.233
8p	9.996*	10.991	0.149	3b₂ → 12a₁	0.91	0.30	-0.995
		10.288	0.021	3b₂ → 8b₂	0.89	0.30	-0.292
9p	10.174*	11.714	0.002	3b₂ → 13a₁	-0.75	0.36	-1.540
		11.646	0.236	3b₂ → 9b₂	0.50	0.44[†]	-1.472
10p	10.263*	11.908	0.376	3b₂ → 14a₁	-0.70	0.40	-1.645
		12.014	0.083	3b₂ → 10b₂	-0.93	0.39	-1.751
4d	8.816	8.957	0.008	3b ₂ → 2a ₂	-0.95	0.17	-0.140
5d	9.613	10.524	0.016	3b₂ → 3a₂	0.89	0.33	-0.910

*blended line, *f*: oscillator strength, *A*: excitation amplitude, Λ : lambda diagnostic

[†]valence-Rydberg mixed nature, O–C: difference of observed and calculated energies

Entries in bold are revised compared to earlier work [4].

Table 4. Vertical excited states of CH₂Br₂ corresponding to Rydberg series converging to IP(2b₁) = 10.74 eV

Assignment	Observed peak position (eV)	Calculated by TDDFT: PBE0/aug-cc-pV5Z					O–C (eV)
		E (eV)	<i>f</i>	Transition	<i>A</i>	Λ	
5s	7.378	7.052	0.059	2b ₁ → 6a ₁	0.91	0.35	0.326
6s	9.275	8.698	0.037	2b ₁ → 8a ₁	-0.86	0.31	0.576
7s	9.831*	9.305	0.001	2b₁ → 10a₁	0.98	0.27	0.526
8s	10.174*	11.062	0.067	2b₁ → 12a₁	-0.91	0.38	-0.888
9s	10.357	11.645	0.039	2b₁ → 13a₁	0.75	0.37	-1.288
5p	8.155	8.089	0.047	2b₁ → 7a₁	0.98	0.27	0.067
		7.847	0.010	2b ₁ → 3b ₁	-0.98	0.22	0.309
6p	9.438*	9.060	0.002	2b₁ → 9a₁	-0.93	0.21	0.378
		8.982	0.005	2b ₁ → 4b ₁	-0.94	0.28	0.456
7p	9.996*	9.852	0.024	2b₁ → 11a₁	0.97	0.29	0.144
		9.456	0.010	2b ₁ → 5b ₁	-0.86	0.25	-0.540
4d	8.983*	9.039	0.128	2b₁ → 2a₂	-0.79	0.29	-0.056
5d	9.791	10.573	0.005	2b₁ → 3a₂	-0.65	0.41[†]	-0.782

*blended line, *f*: oscillator strength, *A*: excitation amplitude, Λ : lambda diagnostic

[†]valence-Rydberg mixed nature, O–C: difference of observed and calculated energies

Entries in bold are revised compared to earlier work [4].

Table 5. Vertical excited states of CH₂Br₂ corresponding to Rydberg series converging to IP(1a₂) = 11.21 eV

Assignment	Observed peak position (eV)	Calculated by TDDFT: PBE0/aug-cc-pV5Z					O–C (eV)
		E (eV)	<i>f</i>	Transition	A	Λ	
5p	8.514	8.240	0.024	1a ₂ → 3b ₁	-0.97	0.19	0.274
		8.525	0.015	1a ₂ → 5b₂	-0.81	0.33	-0.011
6p	9.831	9.290	0.073	1a ₂ → 4b ₁	-0.55	0.29	0.541
		9.335	0.001	1a ₂ → 6b ₂	0.96	0.23	0.497
7p	10.445	9.847	0.004	1a ₂ → 5b ₁	0.84	0.22	0.598
		10.065	0.034	1a ₂ → 7b₂	-0.97	0.24	0.380
8p	10.699	10.408	0.144	1a ₂ → 6b₁	-0.86	0.44[†]	0.291
		10.797	0.105	1a ₂ → 8b ₂	-0.95	0.34	-0.099
4d	9.332	9.413	0.001	1a ₂ → 2a₂	0.65	0.26	0.081
5d	10.263	10.823	0.007	1a ₂ → 3a₂	0.57	0.53[†]	-0.560

f: oscillator strength, A: excitation amplitude, Λ: lambda diagnostic

[†]valence-Rydberg mixed nature, O–C: difference of observed and calculated energies

Entries in bold are revised compared to earlier work [4].

Table 6. Vertical excited states of CH₂Br₂ corresponding to Rydberg series converging to IP(4a₁) = 11.30 eV

Assignment	Observed peak position (eV)	Calculated by TDDFT: PBE0/aug-cc-pV5Z					O–C (eV)
		E (eV)	<i>f</i>	Transition	A	Λ	
5s	7.764	7.609	0.027	4a ₁ → 6a ₁	0.96	0.32	0.155
6s	9.776*	9.195	0.027	4a ₁ → 8a₁	-0.94	0.29	0.580
7s	10.445*	9.825	0.005	4a ₁ → 10a₁	-0.90	0.33	0.619
5p	8.600	8.578	0.023	4a ₁ → 7a ₁	0.91	0.29	0.022
		8.340	<0.001	4a ₁ → 3b ₁	0.96	0.15	0.260
6p	10.079	9.650	0.005	4a ₁ → 9a₁	0.67	0.25	0.429
		9.455	0.027	4a ₁ → 4b ₁	0.94	0.21	-0.624
7p	10.610*	10.405	0.054	4a ₁ → 11a₁	-0.88	0.34	0.205
		9.948	<0.001	4a ₁ → 5b ₁	-0.96	0.17	0.662
8p	10.830	11.524	0.002	4a ₁ → 12a₁	0.91	0.33	-0.694
		10.398	0.001	4a ₁ → 6b ₁	-0.90	0.36	0.431
4d	9.438	9.409	0.056	4a ₁ → 6b₂	0.72	0.29	0.029
5d	10.288	10.146	0.013	4a ₁ → 7b₂	0.97	0.25	0.141
6d	10.679	10.864	0.050	4a ₁ → 8b₂	-0.81	0.32	-0.185

*blended line, *f*: oscillator strength, A: excitation amplitude, Λ: lambda diagnostic

O–C: difference of observed and calculated energies

Entries in bold are revised compared to earlier work [4].

Low lying excited states are typically found to result essentially from single orbital excitations whereas mixing of two or more excitations with comparable amplitude (*A*) becomes more common for high lying excited states (*cf.* Tables 3–6). It is observed that in the case of *np* and *nd*, more than one set of theoretically predicted transitions can be associated with a given experimentally observed series. For example, theoretically predicted transitions corresponding

to $3b_2 \rightarrow 7a_1, 9a_1 \dots$ as well as $3b_2 \rightarrow 5b_2, 6b_2 \dots$ can be assigned to the experimentally observed series $3b_2 \rightarrow np$ (*cf.* Table 3). Similarly, the $2b_1 \rightarrow np$ Rydberg series can be correlated with the theoretically predicted excitations $2b_1 \rightarrow 7a_1, 9a_1 \dots$ as well as $2b_1 \rightarrow 3b_1, 4b_1 \dots$. Although this is possible in principle, more than one series of np/nd type are not resolved in the current set of experiments, therefore both sets of transitions which may be assigned to the np/nd series are included here. Similar trends have been seen in the np/nd series of CH_2Cl_2 and CH_2I_2 [3–5].

(c) Vibronic Structure

Vibronic bands are observed along with several of the Rydberg series. The general methodology used in assignment of the vibronic features is to compare the intervals between successive vibronic bands with the calculated ionic frequencies of CH_2X_2 , which are expected to be closer to the vibrational frequencies in excited Rydberg states [3–5]. Optimized geometries of the dihalomethanes for neutral ground state and cationic ground states computed using DFT are compared in Table 7 along with theoretically predicted vertical and adiabatic ionization energies. A good agreement between the predicted (*cf.* Table 7) and experimental (*cf.* Tables 1 and 2) first IPs validates the appropriateness of the method and basis set used for the molecular systems being studied.

Computed vibrational frequencies for neutral and ionic ground states and assignments of the observed vibronic features have been reported in our earlier papers [3–5], a comparative summary of vibronic assignments is presented here (*cf.* Table 8). A striking feature is that the ν_3 vibration which corresponds to C–X symmetric stretch has been observed in all the three dihalomethanes and forms extensive progressions [3–5]. Additionally in CH_2Cl_2 and CH_2I_2 , the ν_1 (CH sym. stretch), ν_2 (CH_2 bend) and ν_8 (CH_2 wag) modes are also seen [3–5]. The reason for not observing these modes in CH_2Br_2 is not very clear and warrants further investigation. The richest and most extensive vibrational progressions are seen in CH_2Cl_2 , wherein the ν_3 progression could be distinguished up to 9 members in the case of the Rydberg transitions $2b_1 \rightarrow 6p$ and $2b_1 \rightarrow 4p$. Similarly, in Rydberg states of CH_2Br_2 and CH_2I_2 , also, it is the ν_3 mode that is predominantly excited. This indicates a change in geometry in the excited state which involves a change in C–X bond length. Comparing the geometrical parameters in the neutral and ionic ground states (*cf.* Table 7), we find that the predicted changes in the C–X bond lengths are not very large whereas the X–C–X bond angles change appreciably in going from neutral to ionic ground states. This suggests that in excited states of Rydberg nature, the ν_4 mode which involves CX_2 bending should be excited. Similarly, there is a significant change in the H–C–H bond angles, in going from neutral to ionic ground state, for all the three molecules. The corresponding vibrational mode, *i.e.*, ν_2 (CH_2 bend) is observed only in CH_2Cl_2 and CH_2I_2 ; however, it does not give rise to extensive progressions. The non-observance of progressions of the ν_4 mode in all three molecules and the ν_2 mode in CH_2Br_2 may be due to interactions or perturbations not included in the analysis like valence-Rydberg mixing or vibronic coupling with nearby states, a better understanding of which may be gained by higher level *ab initio* calculations. We may also mention here that spin-orbit coupling which becomes more important as we go from Cl to I also should be included in the theoretical treatment in order to obtain a better picture of the excited state electronic and vibrational structure.

Table 7. Optimized ground state geometries of CH₂X₂ and CH₂X₂⁺ using DFT^a

	r(C-X)	r(C-H)	∠(X-C-X)	∠(H-C-X)	∠(H-C-H)	-HOMO + 1 eV	VIE (eV)	AIE (eV)
CH ₂ Cl ₂ ^e	1.761	1.084	112.9	108.1	111.4	9.74	11.29	10.83
	(1.764) ^b	(1.085) ^b	(112.3) ^b	-	(111.9) ^b			
CH ₂ Cl ₂ ^{+e}	1.766	1.086	90.8	111.7	116.5			
CH ₂ Br ₂ ^e	1.922	1.083	113.7	107.8	112.0	9.19	10.38	9.98
	(1.925) ^c	(1.097) ^c	(112.9) ^c	(108.3) ^c	(110.9) ^c			
CH ₂ Br ₂ ^{+e}	1.921	1.084	92.6	111.3	116.5			
CH ₂ I ₂ ^f	2.127	1.082	116.1	107.2	111.9	8.38	9.32	8.96
	(2.12) ^d	(1.09) ^d	(114.7) ^d	-	(111.3) ^d			
CH ₂ I ₂ ^{+f}	2.121	1.084	93.9	111.3	115.8			

^a Experimental values in the parenthesis, ^b Ref. [9], ^c Ref. [10], ^d Ref. [11], ^e PBE0/aug-cc-pV5Z, ^f PBE0/aug-cc-pVQZ

HOMO: highest occupied molecular orbital, VIE: vertical ionization energy, AIE: adiabatic ionization energy

Table 8. Vibrational modes excited along with Rydberg series in the dihalomethanes

Mode	Transitions		
	CH ₂ Cl ₂	CH ₂ Br ₂	CH ₂ I ₂
ν_1	2b ₁ → 5s	–	2b ₁ → 6p
ν_2	2b ₁ → 5s	–	–
ν_3	2b ₁ → 4p	2b ₁ → 5p	2b ₁ → 6s
	2b ₁ → 6p	2b ₁ → 4d	3b ₂ → 6p
	3b ₂ → 4p	3b ₂ → 5p	
	3b ₂ → 5p	3b ₂ → 4d	
ν_8	1a ₂ → 4p	1a ₂ → 5p	
	2b ₁ → 5s	–	2b ₁ → 6p
	2b ₁ → 5p		2b ₁ → 5d
	3b ₂ → 5p		3b ₂ → 6p
$\nu_2 + \nu_8$	–	–	2b ₁ → 6p

4. Conclusions

VUV (6–11.8 eV) photoabsorption spectra of the dihalomethanes CH₂X₂ (X=Cl, Br, I) are compared and correlated to identify similarities, differences and trends in their spectra and excited state structure. The spectra are dominated by Rydberg series of *ns*, *np* and *nd* type which originate from the halogen lone pair non-bonding orbitals, as evident from quantum defect analyses. As we move down the series, from Cl to I, spectral complexity increases due to severe overlap of Rydberg series. Several electronic transitions show associated vibronic structure and are assigned to different vibrational modes. The richest spectra are observed for CH₂Cl₂, both in terms number of Rydberg series members observed as well as extensive vibronic progressions. The major contribution to vibronic structure is from the ν_3 mode (C–X sym. stretch) which appears in all the three molecules and tends to form long progressions. By appropriately taking into account both, the initial and final symmetries of the MOs involved, a revised and improved theoretical versus experimental comparison is presented for CH₂Br₂. We believe that the study presented in this paper will be of interest to augment the spectroscopy and photochemistry of dihalomethanes.

Acknowledgement

Authors acknowledge the help rendered by Dr. B.N. Raja Sekhar and Mr. Vijay Kumar during utilization of the Photophysics beamline, and valuable support by Dr. S.N. Jha and Dr. N.K. Sahoo.

Competing Interests

The authors declare that they have no competing interests.

Authors' Contributions

All the authors contributed significantly in writing this article. The authors read and approved the final manuscript.

References

- [1] T.J. Johnson, T. Masiello and S.W. Sharpe, *Atmos. Chem. Phys.* **6**, 2581 (2006).
- [2] M.B. Robin, *Higher Excited States of Polyatomic Molecules*, Vol. 1 (Academic Press, New York, 1974).
- [3] A. Mandal, P.J. Singh, A. Shastri and B.N. Jagatap, *J. Quant. Spectrosc. Rad. Transfer* **149**, 291 (2014).
- [4] A. Mandal, P.J. Singh, A. Shastri, V. Kumar, B.N.R. Sekhar and B.N. Jagatap, *J. Quant. Spectrosc. Rad. Transfer* **144**, 164 (2014).
- [5] A. Mandal, P.J. Singh, A. Shastri and B.N. Jagatap, *J. Chem. Phys.* **140**, 194312 (2014).
- [6] A. Shastri, B.N. Raja Sekhar, P. Jeet Singh and M.N. Deo, *Spectrosc. Lett.* **42**, 219 (2009).
- [7] P.M.R. Rao, N.C. Das, B.N. Raja Sekhar, S. Padmanabhan, A. Shastri, S.S. Bhattacharya and A.P. Roy, *Nucl. Instr. Meth. Phys. Res. A* **613**, 467-468 (2001).
- [8] M.W. Schmidt, K.K. Baldridge, J.A. Boatz, S.T. Elbert, M.S. Gordon, J.H. Jensen, S. Koseki, N. Matsunaga, K.A. Nguyen, S. Su, T.L. Windus, M. Dupuis and J.A. Montgomery, *J. Comp. Chem.* **14**, 1347 (1993).
- [9] R.J. Berry and M.D. Harmony, *Struct. Chem.* **1**, 49 (1990).
- [10] K. Kuchitsu and G. Graner, *Structure of Free Polyatomic Molecules: Basic Data* (Springer, Berlin, 1998).
- [11] S.A. Kudchadker and A.P. Kudchadker, *J. Phys. Chem. Ref. Data* **4**, 457 (1975).